IEEE Robotics and Automation Letters (RA-L) paper, presented at ICRA 2026, Vienna, Austria. Cite as RA-L paper.

Enhancing Dual-Loop Pressure Control in Pneumatic Soft Robotics with a Comparison of Evolutionary Algorithms for PID & FOPID Controller Tuning

Mostafa Mo. Massoud (*Student Member, IEEE*)[1], Paulo H.T.F Alves (*Student Member, IEEE*) [1], and Jacqueline Libby (*Member, IEEE*)[1]

***Abstract*—The control of pneumatic soft robotics is challenging due to nonlinearites arising from many factors including pneumatic system components and material properties of the soft actuator. Manual methods for PID controller tuning are inadequate for the nonlinear and time-variant dynamics present in soft robotics. Affordable pneumatic components such as on/off valves cause discontinuities in flow rate, introducing nonlinearities and oscillatory fluctuations into the system. This study proposes a dual-loop control system: one for PID and Fractional-Order PID (FOPID) control of a solenoid valve that feeds air into the actuator, and another for PID control of the pump upstream of the valve. The PID and FOPD parameters are optimized using evolutionary algorithms: Genetic Algorithm (GA), Particle Swarm Optimization (PSO), and Simulated Annealing (SA). Simulations and real-world experiments are conducted to validate the optimized parameters. Our results demonstrate that the dual-loop hardware configuration reduces fluctuations from the valves compared with a single-loop control scheme. The experimental statistical analysis confirms that FOPID achieves the highest significant improvements in rise time (PSO) and peak time (GA, PSO), while PID performs better for overshoot (GA, PSO). These findings highlight the importance of selecting an appropriate optimization algorithm based on the specific control objective, as FOPID does not outperform PID in every metric across all methods.**

***Index Terms*—Modeling, Control, and Learning for Soft Robots; Hydraulic/Pneumatic Actuators; Soft Sensors and Actuators; Soft Robot Applications; Sensor-based Control**

I. Introduction

SOFT robots have become popular because they can perform tasks in environments requiring variable stiffness and conformability [1]. Soft actuators are used in applications such as wearable assistive devices [2], locomotion [3], surgical tools [4], and grasping [5]. With an increasing aging population, soft robots are becoming more important in the rehabilitation sector to assist impaired patients [6]. As we have shown in our previous work [7], soft actuators consisting of highly deformable materials can be modeled and fabricated with high accuracy, allowing for great potential in future adaptable designs.

Pneumatics is the most common actuation source for soft robotics due to its easy implementation, environmental friendliness, and good response time [8]. However, pneumatic systems introduce nonlinearities into the control, ontop of the nonlinearities introduced by the deformable materials that the soft actuators are made of. Because pneumatics is the most common actuation mode for soft robotics, many soft robotics researchers have presented open-source pneumatic toolkits to the community, including: Soft Robotics Toolkit (SRT) [9], OpenPneu [10], FlowIO [11], Pneuduino [8], PneuSoRD [12], programmable air [13], and PneuDrive [14]. Pneumatic PWM on solenoid on/off valves is often used to mimic proportional valves. The SRT [9] uses this system in an open-loop configuration, and the OpenPneu kit [10] builds off of this with closed loop control. However, discontinuities in airflow caused by the opening and closing of the valves leads to fluctuations even at steady state. To solve the fluctuation problem, some authors [14] replace the on/off valves with proportional valves. However, proportional valves are more expensive (3–20 times) and heavier (2–5 times) than on/off valves and require more power [15]. The FlowIO kit [11] modulates the motor directly instead of the valves. However, this requires a separate motor for each independently controlled actuator. The authors in [16] implement pneumatic PWM on a pair of 2-way on/off valves, introducing a "hold" state that helps reduce oscillations. Pneusord [12] presents an open source hardware kit that allows for closed-loop control on all of the pneumatic valve configurations discussed above. In comparing the various valve configurations, [12] confirms that proportional valves and pairs of 2-way on/off valves minimize the fluctuations caused by single on/off valves. In addition, they implement a second control loop on the motor to conserve power; however, they do not investigate or exploit other potential benefits of the second control loop, as their main focus is on the valve comparisons. Xavier [17] demonstrates a similar dual closed-loop control configuration, but only in simulation. Building off of this preliminary work in dual closed-loop control, we experimentally demonstrate that the dual-loop control itself

Manuscript received: November, 27, 2024; Revised February, 08, 2025; Accepted April, 05, 2025.

This paper was recommended for publication by Editor C. Laschi upon evaluation of the Reviewers' comments. This work was supported by Stevens Institute of Technology, Department of Mechanical Engineering.

[1]Mostafa Mo. Massoud, Paulo H.T.F Alves, and Jacqueline Libby are with the Department of Mechanical Engineering, Stevens Institute of Technology, Hoboken, NJ 07030 USA. (e-mail: mmassoud@stevens.edu; pteixeir@stevens.edu; jlibby@stevens.edu)

Digital Object Identifier (DOI): see top of this page.

IEEE Robotics and Automation Letters (RA-L) paper, presented at ICRA 2026, Vienna, Austria. Cite as RA-L paper.

can be exploited to reduce oscillations, even with a single on/off valve configuration.

The PID controller is easy to implement and comprehend and is widespread across many industrial applications [18]. Chen [15] applied the PID with two 2-way on/off valves to control the pressure of a soft actuator. Young [12] also used the PID control with a 3-way on/off valve and a proportional valve to control pressure. Huang [19] compared a 2-way on/off valve, a 3-way on/off valve, and a proportional vale when applying a PID controller. Xavier [17] used the PID controller with anti-wind up on a 3-way on/off valve to control pressure. The advanced version of the PID controller is the parallel form of the Fraction Order PID (FOPID) The FOPID provides two additional parameters, which may make it a more robust controller due to its fractional degree structure [20]. Although the FOPID has become a popular controller in robotics applications, it is rarely used for soft robotics [21], [22], [20].

There are several methods for tuning the conventional PID, such as D-partitioning, Ziegler-Nichols, and pole placement [23]. These tuning methods require complete system dynamics and frequency response knowledge and are more suitable for linear and time-invariant systems. Evolutionary optimization algorithms can be used to fine-tune PID parameters of nonlinear soft pneumatic actuator systems [24]. Furthermore, evolutionary algorithms are already the common choice for tuning FOPID time-delayed systems [25], [26]. The Biogeography-Based Optimization algorithm was used for tuning the FOPID of a large-sized pneumatic valve, and the Grey Wolf Optimization (GWO) algorithm was used for tuning the throttle valve position [26]. Evolutionary algorithms use a population of solutions instead of single-point solutions, which reduces their chances of getting caught in local optimum, allowing them to gracefully handle multivariate optimization problems. Although evolutionary algorithms have well-known advantages, they are rarely used for tuning control algorithms in the soft robotics field. This paper addresses that gap by comparing a set of evolutionary algorithms on both PID and FOPID pneumatic controllers for soft actuators. The algorithms compared include: the Genetic Algorithm (GA) [27], Particle Swarm Optimization (PSO) [28], and Simulated Annealing (SA) [29].

This paper presents advances in the pneumatic hardware control system as well as the algorithms to exploit the hardware configurations and optimize the system. Building off of the pneumatic system that we presented in [30], we present two control loops, one for the pump to act like an air compressor and the other for the on/off valve. The pump controller is a PID algorithm with electric PWM on the pump. For the control of the on/off valve, a comparison is made between PID and FOPID algorithms with pneumatic PWM on the valve. The PID and FOPID algorithms are tuned using evolutionary optimization algorithms. The pump control loop aims to maintain the pump pressure slightly above the desired pressure for the valve control loop, which helps to reduce the output fluctuation. In contrast, the valve control loop aims to achieve the desired pressure level exactly and with minimum fluctuations. Three optimization algorithms (GA, PSO, SA) are used with four objective functions (ISE, IAE, ITSE, ITAE) to obtain the tuned parameters for the PID and FOPID controllers for the valve. A comparison between the three optimization algorithms is made in terms of rise time, setting time, percentage of overshoot, peak value, and peak time A Simscape model of the pneumatic toolkit is made with the help of the parameter estimation toolbox. The model is used within the objective functions of the optimization algorithms to obtain the optimized PID and FOID parameters; subsequently, these optimized parameters are used in real-world experiments to validate the simulations.

II. PNEUMATIC SYSTEM DESIGN

The pneumatic system diagram is shown in Fig 1a, which includes two on/off valves (SMC- VQ110U-5M), two pressure sensors (Honeywell-ASDXAVX100PGAA5), a 12ml syringe, a 100ml syringe, and a soft actuator. The corresponding pneumatic diagram is shown in Fig 1b. The configuration uses two control loops, one for the pump and the other for the on/off valve, downstream of the pump. The pump loop uses electrical PWM. The valve loop uses mechanical PWM on the on/off valve. With a typical single-loop control of mechanical PWM on the valve, fluctuations due to the opening and closing of the valves will occur. The pressure source will remain constant, at a value higher than any potential desired value in the scheme. When the desired pressure is low, then the difference between the desired low pressure and the constant high-pressure source will result in a low PWM duty cycle. This means that the PWM duty cycle for the on/off valve will be low-state for a long time and high-state for a short time. In the low state, the valve is exhausting to atmosphere, releasing pressure from the actuator. This pressure drop during the low state will increase the feedback control error, which will then be compensated for in the high state, resulting in an oscillatory fluctuation behavior. To overcome this fluctuation issue, a PID control loop with a 100ml tank is used for the pump to make the pressure source constant and slightly above the desired pressure, which in turn reduces the output fluctuations. The second loop uses the PID and FOPID to control the output pressure through an on/off valve using a PWM signal at 50Hz. A 12ml tank is also used at the output port to reduce the output fluctuations. Lastly, an on/off valve acts as a relief valve to protect the pump from unexpected issues.

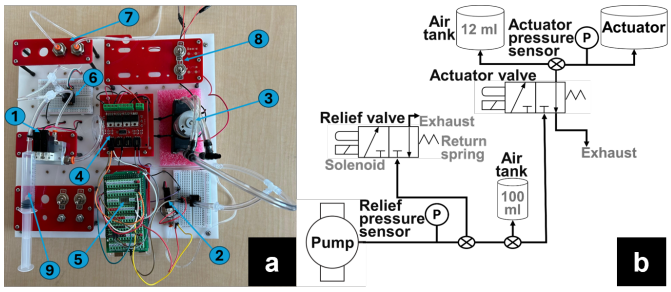

Fig. 1. (a) The Proposed Pneumatic System: 1) on/off Valve, 2) Relief Valve, 3) DC Pump, 4) MOSFET Switches, 5) ATMega2560 Microcontroller, 6) Pressure Sensor, 7) Actuator Outputs, 8) on/off Power Switches, and 9) Syringe [30]. (b) Pneumatic Diagram of the System.

IEEE Robotics and Automation Letters (RA-L) paper, presented at ICRA 2026, Vienna, Austria. Cite as RA-L paper.

Fig. 2 compares the control configurations. The black line is the dual-loop control of both the pump and valve, keeping the pump pressure slightly above the desired value. The green line is a single-loop control of just the pump with electrical PWM, where the valve is kept completely open. The red line is is a single-loop control of just the valve with pneumatic PWM keeping the pump operating continuously with open loop control at a constant pressure. The single-loop control of the valve creates substantial fluctuations, which is unsuitable for low-pressure applications. Single-loop control of the pump minimizes fluctuations and exhibits the best response time; however, such a system requires separate pumps for each independently-controlled actuator, which increases the weight, cost and required power for the system. The dual-loop control of the pump and valve significantly reduces fluctuations and response time. Furthermore, this hardware configuration has the ability to control more than one actuator without requiring an additional pump. Based on this comparison, this paper uses a dual-loop control for the pump and valve to reach the desired pressure with minimum fluctuation and the best response time.

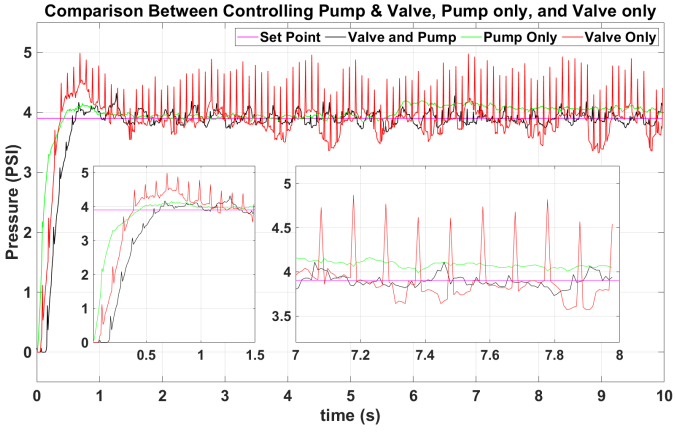

Fig. 2. Control Configurations Comparison

On-off valves introduce nonlinearity in pneumatic systems because they operate in a binary manner, either fully open or fully closed. This leads to sudden jumps in airflow rather than smooth, continuous control.

The volumetric flow rate Q (L/s) through a valve is characterized by the ANSI/(NFPA)T3.21.3 valve model [31]:

$$Q = \frac{114.5 u C_v \sqrt{P_{\text{low}} \Delta P}}{\sqrt{T_{\text{high}}}} \tag{1}$$

where u is the PWM duty cycle, C_v is the flow coefficient, P_{low} is the downstream pressure (bar), ΔP is the pressure difference between upstream and downstream pressure, and T_{high} is the upstream temperature (kelvin).

The pressure dynamics of a single-chamber soft actuator was characterized in [32]:

$$\dot{P}_{spa} = \frac{P_0 Q_{spa}}{V^0_{spa}\left(1 + K_{exp}(2P_{spa} - P_0)\right)} \tag{2}$$

where P_0 is the ambient pressure (0.1 MPA), Q_{spa} is the mass flow rate into the soft actuator, V^0_{spa} is the initial volume of the soft actuator at P_0, K_{exp} is the expansion coefficient, P_{spa} is the current internal pressure of the soft actuator, and $\dot{P}_{spa}$ is the rate of pressure change inside the soft actuator.

When the difference between upstream and downstream pressure, ΔP, increases, the flow rate, Q, increases (eq. 1), resulting in a high pressure change, $\dot{P}_{spa}$, for the soft actuator (eq. 2). To maintain low pressure fluctuation levels in the soft actuator, the rate of pressure change, $\dot{P}_{spa}$, should stay low; therefore, the flow rate, Q, should stay low, and, in turn, ΔP should stay low.

In a single-loop control system (Valve only), the pump pressure level (upstream pressure) is at a constant maximum value. When the actuator pressure (downstream pressure) is low, the difference between upstream and downstream pressure, ΔP, is high, leading to high flow rates and, in turn, high pressure fluctuations. Additionally, when the desired pressure is high and the actuator pressure is low (e.g. in the transient phase of a step response), the high flow rates will lead to pressure overshoot and unstable control. The dual-loop control (Valve and Pump) is presented to overcome fluctuation and overshoot issues by slightly increasing the pump pressure level above the desired pressure level. This keeps ΔP low, which keeps flow rate low.

From an intuitive perspective, we can consider the effect that the valve's ON and OFF times, t_{on} and t_{off}, have on the pressure fluctuations. When the desired pressure is low, the duty cycle is low, and the valve stays OFF for long periods (t_{off} is large). For single-loop control (Valve Only), there will be large pressure fluctuations when the valve turns back ON due to the large pressure difference. In dual-loop control (Valve and Pump), the pressure difference is small, which means a low flow rate to keep the valve ON most of the time. When the valve remains ON almost continuously, it behaves like a proportional valve, smoothing out pressure fluctuations and making the system behave more linearly. This approach minimizes nonlinear effects caused by high flow rates and valve switching, improving overall control performance.

Fig. 2 experimentally validates this theory by comparing the black (dual-loop) and red (single-loop) curves. The standard deviation and peak-to-peak levels of the fluctuation are reduced by 68.28% and 63.03%, respectively, when using the dual-loop control.

Fig. 5 (d,e) compares the dual-loop control's ability to raise and lower a cup of water without spilling, as compared to the single-loop control. This is due to the minimization of pressure fluctuations from the on/off valve. This demonstrates a practical application for the dual-loop control. A video showing the water handling can be viewed in the supplementary material as well as at the following url: https://youtu.be/eZNoIdIQUTI.

III. CONTROL AND OPTIMIZATION METHODOLOGY

Fig. 3 shows the control diagram with an optimization layout. The term "plant" refers to the Simscape model discussed in the next section. In each iteration, the output pressure y(t) is compared to the desired pressure, creating an error signal, which is the input to the controller (PID or FOPID). The

IEEE Robotics and Automation Letters (RA-L) paper, presented at ICRA 2026, Vienna, Austria. Cite as RA-L paper.

controller aims to minimize the error as soon as possible to make the system respond quickly [33], [34]. The discrete PID and FOPID controller equations are:

$$\text{PID:} \quad D[m] = K_P \cdot e[m] + K_I \sum_{i=1}^{m} e[i] \cdot \Delta t_i + K_D \cdot \frac{\Delta e_m}{\Delta t_m} \quad (3)$$

FOPID:

$$D[m] = K_P \cdot e[m] + K_I \sum_{i=1}^{m} e[i] \cdot (\Delta t_i)^{\lambda} + K_D \cdot \frac{\Delta e_m}{(\Delta t_m)^{\mu}} \quad (4)$$

Where m is the number of samples, D[m] is the pneumatic valve duty cycle, e[m] is the difference between the reference and output values, and K_P, K_I, K_D, λ, and μ are the PID and FOPID gains.

The FOPID controller extends the classical PID controller by introducing two additional parameters, λ, and μ, which enhance control flexibility. The λ parameter influences the system's memory of past errors, affecting long-term stability. Increasing λ ($\lambda > 1$) strengthens the integral action, leading to faster steady-state convergence but at the cost of increased overshoot. Similarly, the μ parameter modifies the system's damping characteristics [35]. Higher μ ($\mu > 1$) enhances the derivative action, resulting in a faster rise time but also an increased risk of oscillation. The fine-tuning of λ and μ to achieve an optimal system response is challenging through manual trial-and-error methods, making optimizing algorithms essential for efficiently determining ideal parameter values.

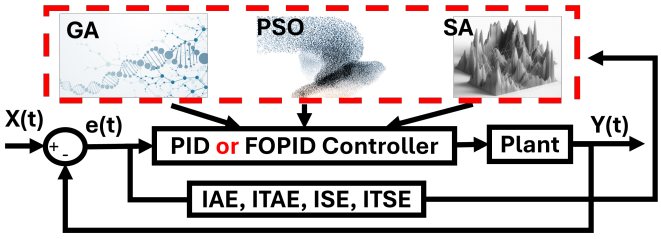

Fig. 3. Control Diagram with Optimization Algorithms

The optimization algorithms (GA, PSO, SA) use the four objective functions (IAE, ISE, ITAE, ITSE) to find the controller gain that achieves the minimum of each objective function. Below are the equations of the four objective functions:

1) Integral Absolute Error (IAE): $IAE = \int_0^{\tau} |e(t)|dt$
2) Integral Time Absolute Error (ITAE): $ITAE = \int_0^{\tau} t|e(t)|dt$
3) Integral Square Error (ISE): $ISE = \int_0^{\tau} |e(t)|^2 dt$
4) Integral Time Square Error (ITSE): $ITSE = \int_0^{\tau} t|e(t)|^2 dt$

The selection of ISE, IAE, ITAE, and ITSE depends on their impact on control performance. ISE prioritizes large errors, leading to fast correction but possible oscillations. IAE treats all errors equally, resulting in a smoother but slower response. ITAE gives more weight to later-stage errors, reducing settling time but causing a slower initial response. ITSE combines ISE and ITAE, balancing response speed and accuracy but potentially amplifying outliers. Since this dual-control approach is suitable for all pneumatic actuators, no single objective function is universally optimal. Engineers select the most suitable one based on system requirements, often comparing multiple functions to achieve the best trade-off.

IV. MODEL OF THE PNEUMATIC SYSTEM

In order to apply the optimization algorithms and validate the experimental results, the Simscape model of the hardware configuration is shown in Fig. 4. There are two control loops, one for the pump and one for the valve. The controller of the valve loop can be PID or FOPID. The magenta colors are pneumatic components, including a flow rate source, two pressure sensors, two syringes, a pipe, a 3/2 solenoid valve, and soft actuators. The soft actuator is modeled as a constant-volume chamber. Noise is modeled as a random noise source block. The pressure source loop aims to simulate the constant pressure source by applying the PID on the flow rate source (diaphragm pump in the real world). The valve control loop seeks to reach the reference valve as soon as possible by applying the PID or FOPID with optimization algorithms to tune the controller parameters.

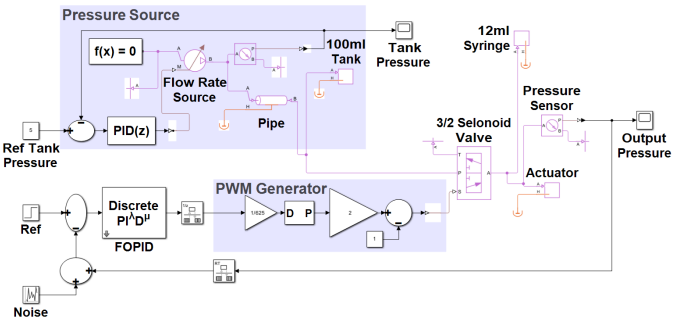

Fig. 4. Simscape Model of the System

V. RESULTS

Table I and Table II show the optimized PID parameters (Kp, Ki, Kd) and FOPID parameters (Kp, Ki, Kd, λ, μ) after running the optimization algorithms (GA, PSO, SA) with the four objective functions (IAE, ITAE, ISE, ITSE), respectively. The optimized parameters are used in simulation and experimental tests to evaluate the PID controller's effectiveness. Fig. 5(a) shows the soft actuator positioned in the test rig used for these experimental tests. The bottom end of the actuator is free to move from bending due to internal pressurization. The top end of the actuator is fixed to the test rig's base, and an inlet tube provides air from the pneumatic control source. The actuator has a pneumatic network (pneunet) geometry and is fabricated from addition-cure silicone with Shore hardness 18A.

Figs. 5(b-e) depict actuators with varying geometries and material properties, all actuated with the same pneumatic control being presented here, demonstating the universality of our algorithms. Fig. 5(d,e) depicts the same soft gripper raising and lowering a beaker of blue-colored water with dual-loop control (d) and single-loop control (e). The water spills with single-loop control due to larger internal air pressure fluctuations, as discussed in Section II with respect to Fig. 2.

IEEE Robotics and Automation Letters (RA-L) paper, presented at ICRA 2026, Vienna, Austria. Cite as RA-L paper.

TABLE I
PID OPTIMIZED PARAMETERS

Algorithm	Objective Function	Objective Function Value	Kp	Ki	Kd
GA	ISE	4.1208	31.2500	499.9693	1.1785
PSO	ISE	4.1207	31.2500	499.9999	1.1781
SA	ISE	4.2829	30.7914	499.9750	2.5555
GA	ITSE	4.4888	31.2500	493.2128	1.1710
PSO	ITSE	4.4821	31.2500	500.0000	1.1773
SA	ITSE	4.4928	30.8081	498.6519	0.7701
GA	IAE	3.5779	31.2500	465.1213	1.1375
PSO	IAE	3.5421	31.2500	500.0000	1.1781
SA	IAE	3.6079	31.0227	449.1603	0.9123
GA	ITAE	12.1794	31.2488	487.2774	2.0281
PSO	ITAE	12.1686	31.2500	500.0000	1.9806
SA	ITAE	12.1852	29.6969	481.9078	2.0319

TABLE II
FOPID OPTIMIZED PARAMETERS

Algorithm	Objective Function	Objective Function Value	Kp	Ki	Kd	λ	μ
GA	ISE	2.9563	31.2500	500.0000	50.0000	0.7250	0.2463
PSO	ISE	2.9563	31.2500	500.0000	50.0000	0.7246	0.2501
SA	ISE	8.6818	11.0000	152.0000	0.0000	1.0000	1.0000
GA	ITSE	4.2801	31.2498	457.2642	49.9995	0.9375	0.1800
PSO	ITSE	4.2421	31.2500	500.0000	50.0000	0.9273	0.1790
SA	ITSE	4.7734	20.3371	203.7302	14.5284	0.9555	-1.4404
GA	IAE	3.2627	31.2500	492.0365	50.0000	0.8607	0.1786
PSO	IAE	3.2523	31.2500	500.0000	50.0000	0.8569	0.1783
SA	IAE	5.1122	11.0000	152.0000	0.0000	1.0000	1.0000
GA	ITAE	12.4743	31.2500	239.1351	0.2103	0.9888	1.5255
PSO	ITAE	12.1236	31.2500	500.0000	50.0000	0.9495	0.0998
SA	ITAE	12.4607	15.2857	198.6619	0.9170	0.9982	-1.8481

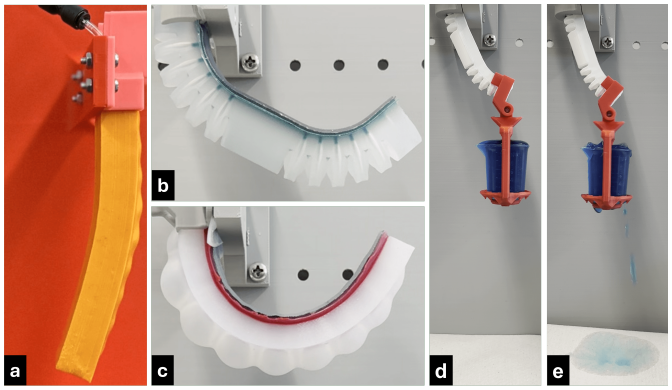

Fig. 5. Soft grippers made with various geometries and materials. (a,b,c,d) Actuated with same dual-loop control. (a) Length 11cm, Shore 18A. (b) Length 11cm, Shore 40A. (c) Length 11cm, Shore 00-50. (d,e) Soft Gripper (length 6cm, Shore 50A) raises and lowers a cup of blue-colored water. (d) Dual-loop control. (e) Single-loop control: **pressure fluctuation causes water spilling.**

A. Simulation Results

Fig. 6 and Fig. 7 illustrate the performance metrics for a pneumatic valve system using PID control, with tuning optimized through three different algorithms: GA, PSO, and SA. Each algorithm was evaluated based on four objective functions: ISE, ITSE, IAE, and ITAE. The GA and PSO generally produced faster rise times than SA across most objective functions except ITSE. GA and PSO achieved lower settling times than SA in the ISE objective function. The SA had the lowest overshoot with ISE but was higher with ITSE. The peak values for pressure and time are closely matched across all algorithms, with slight variations depending on the objective function. Overall, PSO provides a balanced performance regarding response time and overshoot. At the same time, SA offers the best performance in reducing overshoot under certain conditions but at the cost of a longer rise and settling time.

Fig. 6. PID and FOPID Simulation System Response for GA, PSO, SA with IAE, ISE, ITAE, ITSE

Fig. 7. PID Simulation System Response for GA, PSO, SA with IAE, ISE, ITAE, ITSE

Fig. 6 and Fig. 8 illustrate the analogous metrics for FOPID rather than PID. All the responses except for the GA with ITAE objective function are overdamped, so there is no overshoot, peak value, or peak time. GA and PSO generally achieve faster rise times than SA across most objective functions. GA and PSO exhibit similar settling times for most objective functions. SA has a much shorter settling time for the ISE and IAE functions but longer for ITSE.

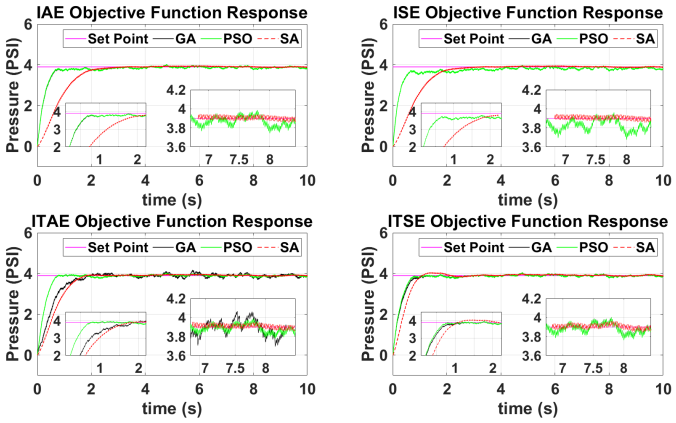

Fig. 8. FOPID Simulation System Response for GA, PSO, SA with IAE, ISE, ITAE, ITSE

B. Experimental Results

1) Step Input: Figs. 9 and 10 illustrate the performance metrics for a pneumatic valve system using PID control, with tuning optimized through three different algorithms: GA, PSO, and SA. Each algorithm was evaluated based on four objective functions: ISE, ITSE, IAE, and ITAE. The PSO consistently produced the fastest rise times across most objective functions. SA followed closely behind, while GA generally exhibited the slowest rise times, mainly with ISE and ITSE objective functions. The PSO with ITAE and SA with ITSE demonstrated the highest settling, while the other algorithms were moderate. The GA with ITAE achieved the lowest overshoot, the PSO with ITAE achieved the highest, while the peak pressure almost constant valve followed the same fashion as the simulation result. The peak time is nearly constant except for GA & PSO with ISE and PSO with IAE.

Figs. 9 and 11 illustrate the analogous experimental metrics for FOPID rather than for PID. GA and PSO generally exhibit lower rise times than SA across most objective functions,

IEEE Robotics and Automation Letters (RA-L) paper, presented at ICRA 2026, Vienna, Austria. Cite as RA-L paper.

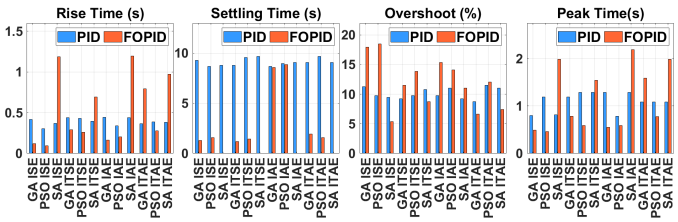

Fig. 9. PID and FOPID Experimental System Response for GA, PSO, SA with IAE, ISE, ITAE, ITSE

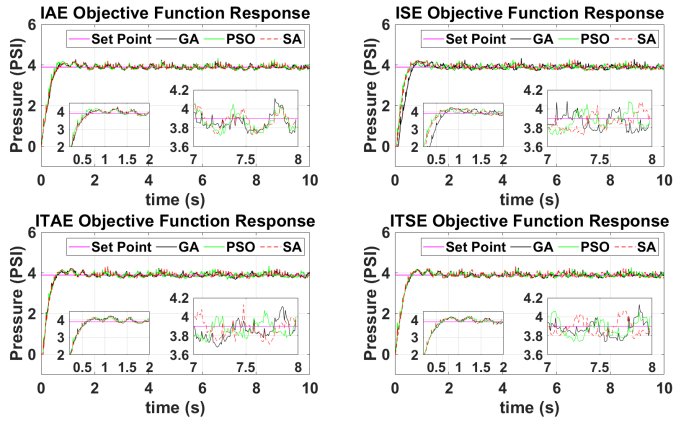

Fig. 10. PID Experimental System Response for GA, PSO, SA with IAE, ISE, ITAE, ITSE

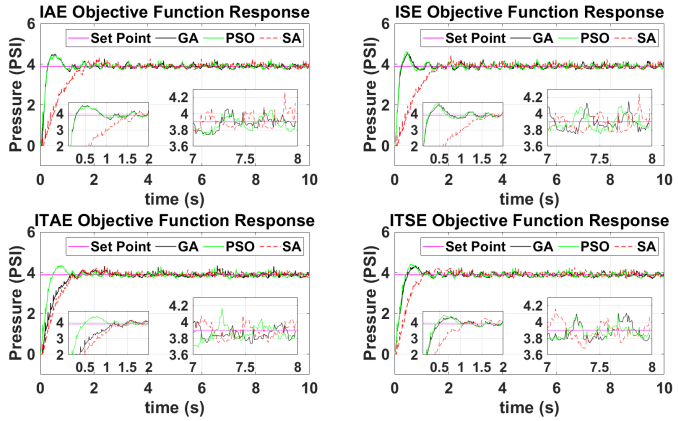

Fig. 11. FOPID Experimental System Response for GA, PSO, SA with IAE, ISE, ITAE, ITSE

which verified the simulation result. GA and PSO have shorter settling times with all objective functions except for the IAE, while SA has NaN value, which refers to the fluctuation at a steady state of more than 5%. PSO tends to produce higher overshoot percentages than GA and SA, particularly in ISE and ITAE. SA shows the lowest overshoot for ISE and ITAE, which may indicate a more conservative tuning but with trade-offs in other areas, such as rise and settling times. Peak pressure values (PSI) and Peak Time vary less dramatically between algorithms but show that PSO often results in slightly higher peak pressures. SA tends to have the highest peak time, particularly under ISE and IAE. GA and PSO perform better in minimizing rise and settling times, with PSO showing higher overshoot. While offering lower overshoot in some cases, SA generally shows higher rise and settling times.

There are some discrepancies between the simulation and experiment results of PID and FOPID Many reasons stand behind thesis discrepancies, such as model simplifications, parameter variations, measurement noise, environmental conditions, and control implementation [36], [37], [38]. For instance, the error of the pressure sensor in this pneumatic system, which includes all errors due to different error sources, can be up to 2% of Full-Scale Span (FSS). Therefore, it may increase the fluctuation around the steady-state value. Finally, the soft actuator is modeled as a constant-volume chamber in the simulation, which is a simplifying assumption that does not take into account the deformation of the soft actuator due to internal pressurization.

Fig. 9 presents a visual summary and comparison of the PID and FOPID experimental results. Certain trends become apparent. For overshoot, PID outperforms the FOPID in most instances. For the other metrics of rise time, settling time and peak time, the FOPID outperforms the PID, except for the SA, where the metric is poor. In particular, for settling time, the FOPID performs drastically better than the PID for the combinations of GA and PSO with the ISE and ITSE objective functions.

2) Step and Sine Wave Inputs: To assess the universality of the proposed control method beyond a single set point, additional experiments were conducted with varying pressure levels. The results, presented in Figs. 12 and 13, illustrate that dual-loop control maintains consistent performance across different operating conditions. This additional validation strengthens the credibility of the approach by demonstrating its real-world applicability in diverse scenarios that require varying pressure levels. Lastly, the new experiments demonstrate that dual-loop control effectively minimizes fluctuations and maintains stability across different pressure levels.

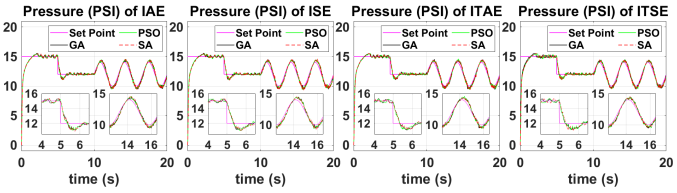

Fig. 12. PID Experimental System Response (Steps + Sine) for GA, PSO, SA with IAE, ISE, ITAE, ITSE

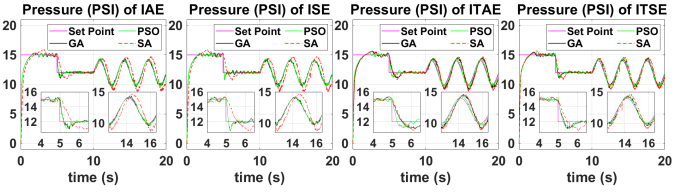

Fig. 13. FOPID Experimental System Response (Steps + Sine) for GA, PSO, SA with IAE, ISE, ITAE, ITSE

3) Statistical Analysis: To ensure statistical reliability, the step input experiments from Section V-B1 are repeated for 30 step values. In Section V-B1, one step value of 4 psi is

IEEE Robotics and Automation Letters (RA-L) paper, presented at ICRA 2026, Vienna, Austria. Cite as RA-L paper.

used with the soft actuator shown in Fig. 5(a). Now 30 step values are sampled from a uniform distribution from [3,18] psi. (20 psi is the pump's maximum). For each of the 30 step samples, we compare PID and FOPID with the ISE objective function across all three optimization algorithms, for a total of 180 experimental trials. The trials are run on the soft actuator shown in Fig. 5(b), which can withstand pressures up to 18 psi since it is made from a stiffer Shore 40A silicone. The results are shown in Fig. 14, using the metrics of rise time, settling time, overshoot, and peak time. Each violin plot shows the distribution of the 30 samples for that controller and optimization algorithm. For each pair of PID and FOPID distributions, a statistical significance test is conducted. The overshoot metric passed a normality test; thus paired-sample t-tests were applied, since the same 30 samples were used as input for the set of experiments. The rise time, settling time, and peak time metrics did not pass normality; thus a Wilcoxon rank-sum test was used.

Each pair of violin plots in Fig. 14 is marked with a bracket, indicating pairwise comparisons between PID and FOPID controllers. Above the brackets, statistical significance is indicated by p-values, with significance levels: ns(not significant), *($p \leq 0.05$), **($0.05 \leq p \leq 0.01$), and ***($0.01 \leq p \leq 0.001$). For almost all metrics, SA performs considerably worse than GA and PSO. Looking more closely at GA and PSO: for peak time, FOPID performs better for both GA and PSO. For settling time, there is no significant difference with either GA or PSO. (Since ISE suffers from bad settling time, it is believable that the statistical tests would be inconclusive for this objective function.) For overshoot, PID performs better for both GA and PSO. For rise time, FOPID performs better for PSO, and for GA, there is no significant difference.

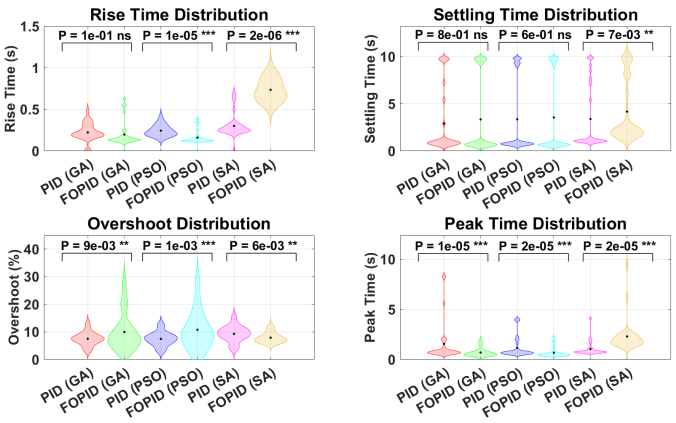

Fig. 14. Violin plots of step response metrics comparing PID and FOPID controllers optimized using GA, PSO, and SA. Brackets indicate pairwise comparisons. Statistical significance is indicated by p-values, with significance levels: ns(not significant), *($p \leq 0.05$), **($0.05 \leq p \leq 0.01$), and ***($0.01 \leq p \leq 0.001$).

The poor performance of the SA in Figs. 9 and 14 can be attributed to SA's inherent limitations in fine-tuning PID/FOPID parameters. Unlike GA and PSO, which leverage population-based search mechanisms for continuous refinement, SA follows a single-solution stochastic approach [39], making it more prone to premature convergence and suboptimal tuning. Additionally, SA's performance is highly sensitive to the cooling schedule and initial conditions [40], which may explain its inferior results. These factors collectively result in weaker PID/FOPID parameter tuning, leading to less effective control performance.

VI. Conclusion

This study explored the application of evolutionary algorithms (GA, PSO, SA) for optimizing PID and FOPID controllers in pneumatic soft robotic systems. The research addressed the challenges of nonlinearities and fluctuations in pneumatic actuation by implementing dual control loops: one for maintaining pump pressure using PID and another for precise pressure control of on/off valves using PID and FOPID tuned by the selected algorithms.

The statistical analysis shows that FOPID significantly improves peak time across all optimization methods except the SA, while also achieving notable improvements in rise time (PSO). However, no significant difference was found in the rise time for GA and settling time for GA and PSO, indicating that the performance benefits of FOPID depend on both the optimization method and the specific performance metric being analyzed. These results emphasize the need for careful optimization strategy selection to achieve the best trade-offs in controller performance. This work significantly contributes to soft robotics by enhancing control precision and stability in pneumatic systems, thereby supporting more advanced and reliable robotic applications. Future research could apply ranking algorithms [41] to select the best response according to the application and then explore the integration of other advanced control strategies.

References

[1] Jianshu Zhou, Shu Chen, and Zheng Wang. A soft-robotic gripper with enhanced object adaptation and grasping reliability. *IEEE Robotics and Automation Letters*, 2(4):2287–2293, 2017.

[2] Pham H. Nguyen, I. B. Imran Mohd, Curtis Sparks, Francisco L. Arellano, Wenlong Zhang, and Panagiotis Polygerinos. Fabric soft polylimbs for physical assistance of daily living tasks. In *2019 International Conference on Robotics and Automation (ICRA)*, pages 8429–8435, 2019.

[3] Nicholas W. Bartlett, Michael T. Tolley, Johannes T. B. Overvelde, James C. Weaver, Bobak Mosadegh, Katia Bertoldi, George M. Whitesides, and Robert J. Wood. A 3d-printed, functionally graded soft robot powered by combustion. *Science*, 349(6244):161–165, 2015.

[4] Max McCandless, Alexander Perry, Nicholas DiFilippo, Ashlyn Carroll, Ehab Billatos, and Sheila Russo. A soft robot for peripheral lung cancer diagnosis and therapy. *Soft Robotics*, 9(4):754–766, 2022. PMID: 34357810.

[5] Changhyun Choi, Wilko Schwarting, Joseph DelPreto, and Daniela Rus. Learning object grasping for soft robot hands. *IEEE Robotics and Automation Letters*, 3(3):2370–2377, 2018.

[6] Hong Kai Yap, Phone May Khin, Tze Hui Koh, Yi Sun, Xinquan Liang, Jeong Hoon Lim, and Chen-Hua Yeow. A fully fabric-based bidirectional soft robotic glove for assistance and rehabilitation of hand impaired patients. *IEEE Robotics and Automation Letters*, 2(3):1383–1390, 2017.

[7] Jacqueline Libby, Aniket A Somwanshi, Federico Stancati, Gayatri Tyagi, Aadit Patel, Naigam Bhatt, JohnRoss Rizzo, and S Farokh Atashzar. What happens when pneu-net soft robotic actuators get fatigued? In *IEEE International Symposium on Medical Robotics*, Atlanta, GA, April 2023.

[8] Matheus S. Xavier, Charbel D. Tawk, Ali Zolfagharian, Joshua Pinskier, David Howard, Taylor Young, Jiewen Lai, Simon M. Harrison, Yuen K. Yong, Mahdi Bodaghi, and Andrew J. Fleming. Soft pneumatic actuators: A review of design, fabrication, modeling, sensing, control and applications. *IEEE Access*, 10:59442–59485, 2022.

IEEE Robotics and Automation Letters (RA-L) paper, presented at ICRA 2026, Vienna, Austria. Cite as RA-L paper.

[9] Dónal P. Holland, Evelyn J. Park, Panagiotis Polygerinos, Gareth J. Bennett, and Conor J. Walsh. The soft robotics toolkit: Shared resources for research and design. *Soft Robotics*, 1(3):224–230, 2014.

[10] Yingjun Tian, Renbo Su, Xilong Wang, Nur Banu Altin, Guoxin Fang, and Charlie C. L. Wang. Openpneu: Compact platform for pneumatic actuation with multi-channels. In *2023 IEEE/ASME International Conference on Advanced Intelligent Mechatronics (AIM)*, pages 765–770, 2023.

[11] Ali Shtarbanov. Flowio development platform – the pneumatic "raspberry pi" for soft robotics. In *Extended Abstracts of the 2021 CHI Conference on Human Factors in Computing Systems*, CHI EA '21, New York, NY, USA, 2021. Association for Computing Machinery.

[12] Taylor R. Young, Matheus S. Xavier, Yuen K. Yong, and Andrew J. Fleming. A control and drive system for pneumatic soft robots: Pneusord. In *2021 IEEE/RSJ International Conference on Intelligent Robots and Systems (IROS)*, pages 2822–2829, 2021.

[13] Amitabh Shrivastava. Programmable air. https://www.programmableair.com/, 2024. Accessed: 2024-08-30.

[14] Curtis C. Johnson, Daniel G. Cheney, Dallin L. Cordon, and Marc D. Killpack. Pneudrive: An embedded pressure control system and modeling toolkit for large-scale soft robots. In *2024 IEEE 7th International Conference on Soft Robotics (RoboSoft)*, pages 786–792, 2024.

[15] Peng Chen, Qing Ding, Yuwang Liu, Zhaoyan Deng, and Jiajia Huang. Programmable pressure control in pneumatic soft robots with 2-way 2-state solenoid valves. *IEEE Robotics and Automation Letters*, 9(7):6448–6455, 2024.

[16] Joran W. Booth, Jennifer C. Case, Edward L. White, Dylan S. Shah, and Rebecca Kramer-Bottiglio. An addressable pneumatic regulator for distributed control of soft robots. In *2018 IEEE International Conference on Soft Robotics (RoboSoft)*, pages 25–30, 2018.

[17] Matheus S. Xavier, Andrew J. Fleming, and Yuen K. Yong. Design and control of pneumatic systems for soft robotics: A simulation approach. *IEEE Robotics and Automation Letters*, 6(3):5800–5807, 2021.

[18] Adeel Ahmad Jamil, Wen Fu Tu, Syed Wajhat Ali, Yacine Terriche, and Josep M. Guerrero. Fractional-order pid controllers for temperature control: A review. *Energies*, 15(10), 2022.

[19] Haiming Huang, Junhao Lin, Linyuan Wu, Bin Fang, and Fuchun Sun. Optimal control scheme for pneumatic soft actuator under comparison of proportional and pwm-solenoid valves. *Photonic Network Communications*, 37:153–163, 2019.

[20] Nie Zhuo-Yun, Zheng Yi-Min, Wang Qing-Guo, Liu Rui-Juan, and Xiang Lei-Jun. Fractional-order pid controller design for time-delay systems based on modified bode's ideal transfer function. *IEEE Access*, 8:103500–103510, 2020.

[21] Mohd Iskandar Putra Azahar, Addie Irawan, and R.M.T. Raja Ismail. Adjustable convergence rate prescribed performance with fractional-order pid controller for servo pneumatic actuated robot positioning. *Cognitive Robotics*, 3:93–106, 2023.

[22] Jorge Muñoz, Raúl de Santos-Rico, Lisbeth Mena, and Concepción A. Monje. Humanoid head camera stabilization using a soft robotic neck and a robust fractional order controller. *Biomimetics*, 9(4), 2024.

[23] M. Abdelbar, Huda Ramadan, Abdelrahman Khalil, Hamad Farag, Mazen Bahgat, Omar Rabie, and Yasser El-Shaer. Optimization of pi-cascaded controller's parameters for linear servo mechanism: A comparative study of multiple algorithms. *IEEE Access*, 11:86377–86396, 2023.

[24] Stephen Bassi Joseph, Emmanuel Gbenga Dada, Afeez Abidemi, David Opeoluwa Oyewola, and Ban Mohammed Khammas. Metaheuristic algorithms for pid controller parameters tuning: review, approaches and open problems. *Heliyon*, 8(5):e09399, 2022.

[25] Aykut Fatih Güven and Onur Özdal Mengi. Nature-ınspired algorithms for optimizing fractional order pid controllers in time-delayed systems. *Optimal Control Applications and Methods*, 45(3):1251–1279, 2024.

[26] Mohamed Jasim Mohamed and Luay Thamir Rasheed. Design of nonlinear pid and fopid controllers for electronic throttle valve plate's position. *Journal of Electrical and Computer Engineering*, 2024(1):9984750, 2024.

[27] John H. Holland. *Adaptation in natural and artificial systems*. University of Michigan Press, Ann Arbor, 1975.

[28] Tareq M. Shami, Ayman A. El-Saleh, Mohammed Alswaitti, Qasem Al-Tashi, Mhd Amen Summakieh, and Seyedali Mirjalili. Particle swarm optimization: A comprehensive survey. *IEEE Access*, 10:10031–10061, 2022.

[29] S. Kirkpatrick, C. D. Gelatt, and M. P. Vecchi. Optimization by simulated annealing. *Science*, 220(4598):671–680, 1983.

[30] Mostafa M. Massoud and Jacqueline Libby. Comparative analysis of evolutionary algorithms for pid controller optimization in pneumatic soft robotic systems: A simulation and experimental study. *IEEE Access (accepted)*, oct 2024.

[31] Matheus S. Xavier, Andrew J. Fleming, and Yuen K. Yong. Model-based nonlinear feedback controllers for pressure control of soft pneumatic actuators using on/off valves. *Frontiers in Robotics and AI*, 9, 2022.

[32] Sagar Joshi and Jamie Paik. Pneumatic supply system parameter optimization for soft actuators. *Soft Robotics*, 8(2):152–163, 2021. PMID: 32598232.

[33] Mostafa Mo. Massoud, A. Abdellatif, and Mostafa R. A. Atia. Different path planning techniques for an indoor omni-wheeled mobile robot: Experimental implementation, comparison and optimization. *Applied Sciences*, 12(24), 2022.

[34] M. Massoud, A. Abdellatif, and Mostafa R. A. Atia. Mechatronic design and path planning optimization for an omni wheeled mobile robot for indoor applications. In *2021 31st International Conference on Computer Theory and Applications (ICCTA)*, pages 90–98, 2021.

[35] Yuxin He, Aixiang Ma, Yuehui Wang, Xinyi Tian, and Sihai Zhao. Fopid controller design for pneumatic control valves with ultra-low overshoot, rapid response and enhanced robustness. *Scientific Reports*, 15(1):4541, 2025.

[36] Peng Zhang, Xu Qiang, Yang Chunhao, Ma Wuning, and Zhang Zhendong. Simulation and experimental investigation of high-pressure pneumatic pilot-driven on/off valve with high transient performances for compressed air ejection. *Flow Measurement and Instrumentation*, 94:102466, 2023.

[37] Qihui Yu, Jianwei Zhai, Qiancheng Wang, Xuxiao Zhang, and Xin Tan. Experimental study of a new pneumatic actuating system using exhaust recycling. *Sustainability*, 13(4), 2021.

[38] Aixiang Ma, Heruizhi Xiao, Xihao Yan, Xianghao Kong, Feng Rong, Lu Zhang, and Sihai Zhao. Simulation and experimental study of a novel negative-pressure flapper–nozzle mechanism. *Micromachines*, 15(1), 2024.

[39] Mihailo Micev, Martin Ćalasan, Ziad M. Ali, Hany M. Hasanien, and Shady H.E. Abdel Aleem. Optimal design of automatic voltage regulation controller using hybrid simulated annealing – manta ray foraging optimization algorithm. *Ain Shams Engineering Journal*, 12(1):641–657, 2021.

[40] Kambiz Shojaee G., Hamed Shakouri G., and Mojtaba Behnam Taghadosi. Importance of the initial conditions and the time schedule in the simulated annealing. In Rui Chibante, editor, *Simulated Annealing*, chapter 12. IntechOpen, Rijeka, 2010.

[41] Mostafa Mohammed Massoud Hamd, Ahmed Abdellatif Hamed Ibrahim, and Mostafa Rostom Ahmed Atia. Selecting dynamic path planning algorithm based-upon ranking approach for omni-wheeled mobile robot. *Journal of Advanced Research in Applied Sciences and Engineering Technology*, 41(2):125–138, Mar. 2024.